Carbohydrate Research, 180 (1988) 87–95
Elsevier Science Publishers B.V., Amsterdam – Printed in The Netherlands

PHYSICOCHEMICAL CHARACTERIZATION OF INULIN AND SINISTRIN*

WOLF-DIETER EIGNER, PETER ABUJA,
Institut für Physikalische Chemie, Karl-Franzens-Universität Graz, Heinrichstraße 28, A-8010 Graz (Austria)

ROLAND H. F. BECK, AND WERNER PRAZNIK
Institut für Chemie, Universität für Bodenkultur, Gregor-Mendel-Straße 33, A-1180 Wien (Austria)

(Received August 14th, 1987; accepted for publication, January 8th, 1988)

ABSTRACT

Inulin and sinistrin were investigated by low angle laser light scattering coupled with size-exclusion chromatography (s.e.c.-l.a.l.l.s.) and by dynamic light scattering (d.l.s.) in order to obtain molecular weights, molecular-weight distributions, and hydrodynamic radii. Small angle X-ray scattering (s.a.x.s.) experiments were carried out for the determination of the radii of gyration. In addition model calculations using the s.a.x.s. data provided information on the geometry of the molecules. The results indicate a rod-like shape for inulin whereas sinistrin appears to be more spherical in aqueous solution. As the two polysaccharides do not differ significantly in molecular weight and volume, but show a distinct difference in their maximum dimensions, the branched sinistrin must be somewhat more compact than inulin.

INTRODUCTION

Fructans are widely distributed reserve polysaccharides occurring in dicotyledonous plants as the strictly linear β-(2→1)-linked inulin[1],

→1)-β-D-Fru*f*-(2→1)-β-D-Fru*f*-(2↔1) α-D-Glc*p*

and in monocotyledonous plants as the branched β-(2→1),β-(2→6)-linked fructans[2].

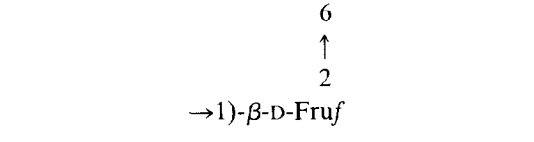

*Presented at the 4th European Carbohydrate Symposium, Darmstadt, F.R.G., July 12–17, 1987.

0008-6215/88/$ 03.50

Moreover, there exist bacterial fructans (levans), mostly β-(2→6)-linked, which play an important role in phytopathological infection processes[3] and in plaque formation by cariogenic bacteria[4]. Plant fructans are usually stored supersaturated in the vegetative organs, where they can influence the osmotic pressure and the freezing point of cells[5]. Compared with starch, the biosynthesis of fructans does not require activated sugar nucleotides and is therefore less energy-consuming[6]. The enzymes involved in this process transfer fructose moieties directly from sucrose to 1-kestose (fructosylsucrose) and to higher polymers. That is why fructans are terminated at their "reducing" end by glucose and are not reducing. Clearly the correct chemical term — which is not commonly used — would be glucofructan.

In the present work we chose commercially available sinistrin as an example of a branched fructan. Sinistrin is water soluble at room temperature whereas inulin remains nearly insoluble in cold water and thus requires heating for dissolution. Inulin and sinistrin are utilized for the determination of renal clearance, as both polysaccharides are filtered in the kidney through the glomeruli only and neither reabsorbed nor secreted by the cells of the tubuli[7]. The aim of this work was to characterize the two polysaccharides by different physico-chemical methods in order to explain the distinct behavior and typical qualities of linear and branched low-molecular-weight polysaccharides. Another important aspect is the employment of inulin and sinistrin as model substances for studying the more complex amylose and amylopectin.

EXPERIMENTAL

Materials. — Inulin was prepared from Jerusalem artichoke tubers and purified by two crystallizations from water[8]. Sinistrin, isolated from red squill[2], was a product of Laevosan GmbH, Linz, Austria.

Size-exclusion chromatography. — Size-exclusion chromatography was coupled with a low angle laser light scattering instrument (Chromatix KMX-6, LDC/Milton Roy) (s.e.c.-l.a.l.l.s. technique)[9-11]. A differential refractometer (Refracto Monitor III, LDC/Milton Roy) was used as a concentration-sensitive detector. Inulin and sinistrin were dissolved in fresh distilled water and chromatographed on a Superose 12 column (Pharmacia) at a flow rate of 0.6 mL/min. The inulin samples had to be heated to obtain clear solutions. The sample concentration for s.e.c.-l.a.l.l.s. experiments was 10 mg/mL using a loop volume of 200 μL.

Data acquisition was managed by an IBM-compatible personal computer equipped with an analog-to-digital converter. The stored data were processed by a program specially written for s.e.c.-l.a.l.l.s. data analysis. The error introduced by chromatographic dispersion effects occurring in the column and in the detector cells does not affect the computed weight-average molecular weight ($\overline{M}_w$). The calculated number-average molecular weight ($\overline{M}_n$) is somewhat greater than the true value. However, a comparison of the number-average molecular weight of inulin obtained from s.e.c.-l.a.l.l.s. experiments with data from osmometric meas-

urements showed a deviation less than 2%. Hence a deconvolution of the experimental chromatograms was not necessary.

The specific refractive increment (dn/dc) was determined on a Brice Phoenix differential refractometer equipped with a 632.8 nm interference filter to isolate the wavelength produced by a helium–neon laser. For inulin and sinistrin the same specific refractive increment was found, namely, $dn/dc = 0.143$ mL/g.

Static l.a.l.l.s. — In addition to s.e.c.-l.a.l.l.s. experiments, static l.a.l.l.s. measurements were carried out at the same low forward angle (4.9°) to get the weight-average molecular weight ($\overline{M}_w$), and the second virial coefficient (A_2), which has to be known for s.e.c.-l.a.l.l.s. data analysis.

Dynamic light scattering (d.l.s.). — Dynamic light scattering experiments were performed with a laser spectrometer/goniometer (ALV-SP81, ALV-GmbH, Langen, F.R.G.). An argon ion laser (Spectra Physics, model 2020-03) operating at 500 mW in the single-line mode (selected wavelength 514.5 nm) served as the light source. The detected signal was digitized by means of a preamplifier-discriminator built into the photomultiplier. The digitized signal was then fed to an autocorrelator (Langely–Ford, model 64). The correlation function was analyzed according to the method of cumulants[12]. Samples, at concentrations up to 10 mg/mL, were filtered directly into a cylindrical cuvette through a membrane filter (cellulose acetate, 0.2 μm pore size). All light scattering experiments (l.a.l.l.s. and d.l.s.) were performed at room temperature.

Small angle X-ray scattering (s.a.x.s.). — Small angle X-ray scattering experiments were done with a Kratky camera (improved compact type) with slit-collimation system, on a Philips PW1730 X-ray generator having a copper tube, operated at 50 kV and 30 mA. Each scattering curve was recorded up to 7 times over the range $\mathbf{h} = 0.1$ to 5.1 nm^{-1} [$\mathbf{h}$, the scattering vector $= (4\pi/\lambda) \cdot \sin\theta$, where 2θ is the scattering angle and λ is 0.154 nm, the wavelength of the Cu$K\alpha$ line]. The temperature of the measurement was 4°. The data were averaged and the results extrapolated to zero concentration. Data evaluation, desmearing, and indirect Fourier transformation were done as described by Glatter and Kratky[13,14].

RESULTS AND DISCUSSION

From s.e.c.-l.a.l.l.s. experiments the weight-average molecular weight, $\overline{M}_w$, of sinistrin deviates very little from the value for inulin, as can be seen in Table I. The polydispersity of sinistrin turned out to be about 10% higher than that of inulin. Nevertheless both polysaccharides could be regarded as only moderately polydisperse, since the differential molecular-weight-distribution curves of both had a gaussian shape (see, for example, Fig. 2). Our molecular weight data for inulin are in good agreement with those given by Phelps[15], whereas our values for sinistrin proved to be somewhat higher than those determined by Nitsch *et al.*[2].

Performance of static l.a.l.l.s. experiments in order to obtain the weight-average molecular weight of the bulk polysaccharide provided much higher $\overline{M}_w$-values.

TABLE I

MOLECULAR WEIGHTS OF INULIN AND SINISTRIN FROM S.E.C.-L.A.L.L.S. AND STATIC L.A.L.L.S. EXPERIMENTS

Sample	$\overline{M}_w$	$\overline{M}_n$	$\overline{M}_w/\overline{M}_n$
Inulin			
S.e.c.-l.a.l.l.s[a]			
Main peak only	7200 ±100	6100 ±500	1.18
Prepeak included	11600		
Static l.a.l.l.s.	11500 ±500		
Sinistrin			
S.e.c.-l.a.l.l.s.[a]	6700 ±300	5200 ±300	1.29
Static l.a.l.l.s.	9200 ±600		

[a]The values from the s.e.c.-l.a.l.l.s. experiments represent averages of at least 5 runs.

The reason for the considerable difference is probably the presence of small amounts of impurities — obviously pectins — as one can clearly see in Fig. 1. Here the l.a.l.l.s. response shows a distinct prepeak at a retention volume coinciding with the exclusion limit of the s.e.c.-column. This prepeak was found for sinistrin, too. There is no significant reponse from the refractive-index detector, which means that the concentration of the responsible impurities must be lower than 1%. Because the scattering intensity is proportional to the sixth power of the particle dimension, a few very large particles will scatter even more than the bulk of very small particles. In such cases the static l.a.l.l.s. readings will lead to higher calculated weight-average molecular weights. Including the prepeak in the processing of the s.e.c.-l.a.l.l.s. data yielded the same $\overline{M}_w$-value as determined with static l.a.l.l.s.

Dynamic light scattering (d.l.s.) was done to learn the hydrodynamic radii R_h from the translational diffusion behavior of inulin and sinistrin. This entity — together with the radius of gyration R_g obtainable from s.a.x.s. experiments — permits estimations of the compactness of a molecule, and the degree to which it may be regarded as spherical. In Table II the hydrodynamic radii R_h — computed from

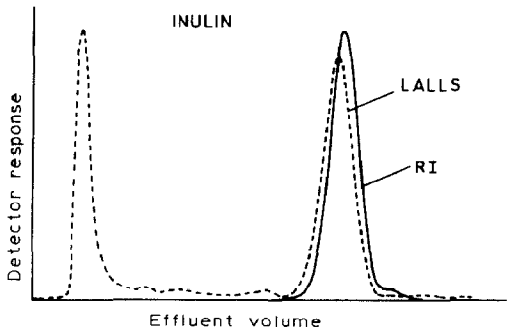

Fig. 1. Typical s.e.c.-l.a.l.l.s. signal of inulin. Solid line shows response of refractive index detector. The prepeak sensed by the l.a.l.l.s. detector is due to impurities, presumably pectins.

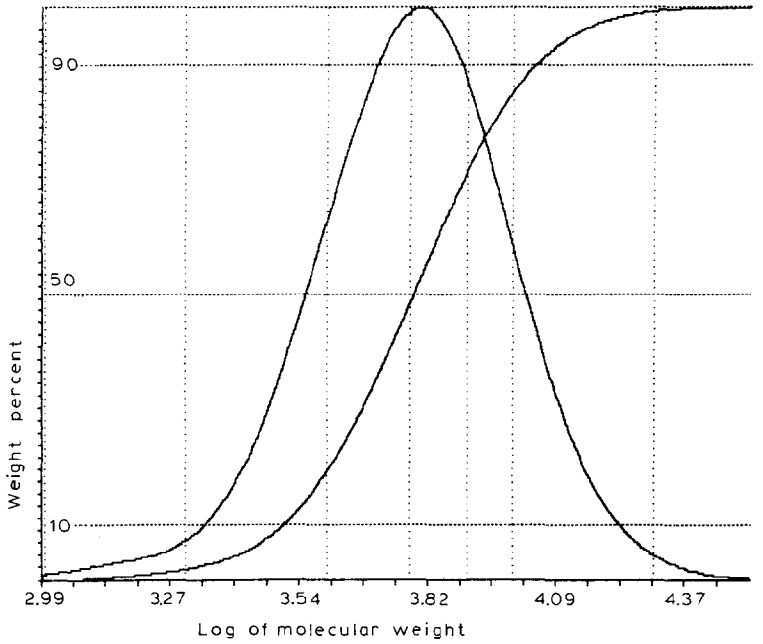

Fig. 2. Differential and cumulative molecular weight distribution for sinistrin.

the translational diffusion constants via the Stokes–Einstein equation — are listed. The fresh inulin as well as sinistrin samples do not differ very much in hydrodynamic size for measurements at a scattering angle, θ, of 90°. For inulin measurements were also performed at $\theta = 30°$. The hydrodynamic radius of the fresh sample proved to be a little larger, as d.l.s. experiments on such small particles are more

TABLE II

HYDRODYNAMIC RADII OF INULIN AND SINISTRIN FROM D.L.S. EXPERIMENTS

Sample	R_h *(nm)*[a]
Inulin	
Measured at $\theta = 90°$	
Fresh sample	1.92 ±0.08
After 48 h	2.09 ±0.06
Measured at $\theta = 30°$	
Fresh sample	2.08 ±0.21
After 48 h	3.65 ±0.58
Sinistrin	
Measured at $\theta = 90°$	
Fresh sample	1.89 ±0.09
After 48 h	1.90 ±0.09

[a]Average values, computed in each case from 10 independent runs.

affected by the presence of even a small amount of aggregates or dust particles at lower scattering angles. For a 48-hour old inulin sample this effect became more drastic; then the hydrodynamic radius increased even at $\theta = 90°$. At $\theta = 30°$ the radius changed dramatically, and there was a considerable increase in the standard deviation. The data for sinistrin remained constant over the same time span, and thus one can suppose that the change in the hydrodynamic size of inulin resulted from some aggregation or retrogradation of the inulin molecules in aqueous solution.

Small angle X-ray scattering experiments were performed on a series of samples at 4 concentrations ranging from 25 mg/mL to 100 mg/mL for both inulin and sinistrin. At these high concentrations samples remained stable for days in the case of sinistrin, whereas inulin samples were not stable for more than 24 hours. Despite these experimental impediments the quality of the inulin data met, to a reasonable extent, the requirements for an extrapolation to zero concentration. In Table III the results from the s.a.x.s. experiments are summarized. Although the hydrodynamic radius was the same for fresh inulin and sinistrin, the radius of gyration R_g was found to be significantly smaller for sinistrin. Considering the p(r) function (see Figs. 3 and 4) the D_{max} value — which corresponds to the maximum dimension of the particle — is about 20% larger for inulin. Consequently, to obtain some idea about the shape of inulin and sinistrin, model calculations were performed. These were done with the MULTIBODY program[16], which permits the calculation of the p(r) and I(h) functions of models constructed from arbitrary spheres. These functions were compared with the experimental ones. Usually the fit of the p(r) function is regarded as the major criterion for the quality of the model, as the I(h) function at larger angles is often influenced by minor variations in electron density which cannot be reconstructed because of the resolutional limitations of the method. We think the fit reasonably good if the model p(r) is situated well inside the error band of the experimental p(r) function, which means that the model precision is in the order of experimental error. The radii of the spheres in the calculations were 0.19 nm for sinistrin and 0.20 nm for inulin. These

TABLE III

RESULTS FROM S.A.X.S. EXPERIMENTS AND MODEL CALCULATIONS

	Inulin	*Sinistrin*
R_g (nm)	1.76 ±0.08	1.54 ±0.06
D_{max} (nm)	7.10 ±0.70	6.00 ±0.60
Model dimensions		
Length (nm)	5.9	5.1
Average diameter (nm)	1.6	1.7
Max. diameter (nm)	2.3	2.5
V (nm^3)	12.8	12.3

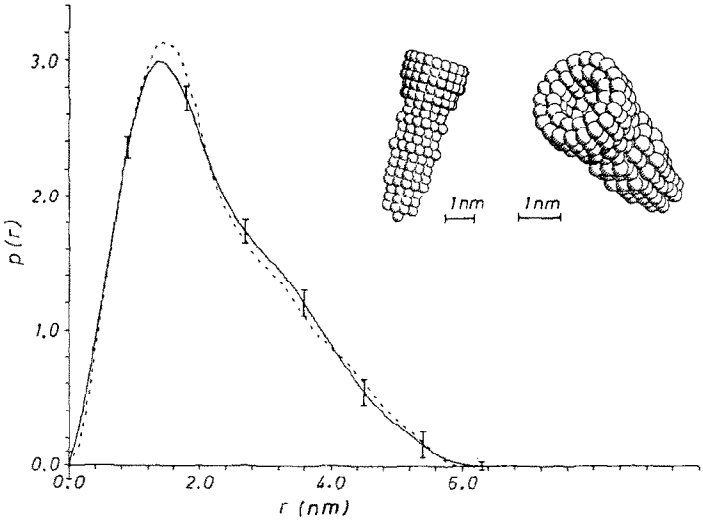

Fig. 3. The p(r) function of inulin. The parameter r is the electron pair distance in nm; p(r) is given in arbitrary units. The solid line represents the experimental data, with computed error bars. The dotted line shows the p(r) function calculated for the best fitting model, which is presented in the figure.

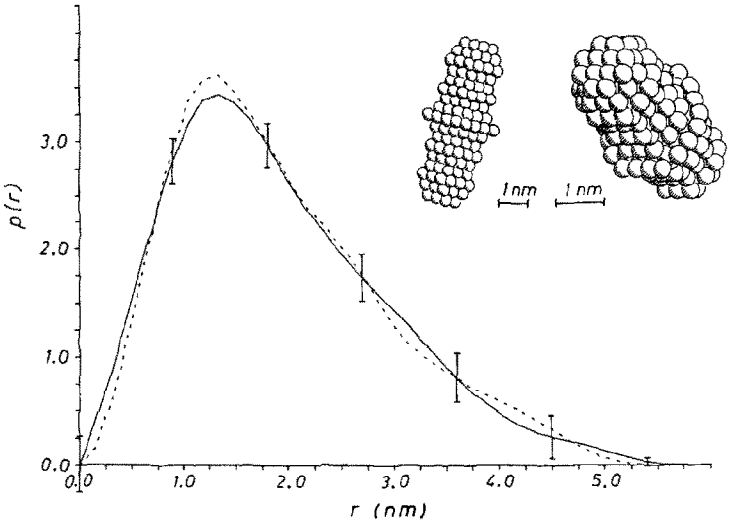

Fig. 4. The p(r) function of sinistrin. As in Fig. 3 the dotted line represents the p(r) function calculated for the best fitting model, shown in the figure. The shoulders reflect the substructure due to the use of a finite number of spheres for the modelling. The position of the shoulders might be shifted to some extent if spheres of a different size were assumed.

spheres have no connection whatsoever with the internal substructure, but are only utilized as a sort of modelling clay. Equally weighted spheres were employed to get a uniform "electron density" within the model. Other than that, the spheres were used to generate a mass distribution comparable to the experimental $p(r)$, especially in the case of sinistrin, which we assume to have a rather "spongy" structure.

For inulin the maximum model dimensions are 5.9 × 1.6 nm (length × mean diameter), for sinistrin 5.1 × 1.7 nm. The volumes may be computed from the sum of the volumes of the spheres and this result for inulin is 12.8 nm^3, for sinistrin 12.3 nm^3. The overall shape for inulin resembles a truncated cone with diameters ranging from about 1.2 to 2.3 nm, and a funnel-shaped thicker end. Compared with this "spaceship"-like shape of inulin, sinistrin may be regarded as a prolate ellipsoid or "dumpling" having a distinct girdle of diameter 2.5 nm.

CONCLUSIONS

Summarizing all the experimental data we are led to following conclusions:

(a) There is no significant difference in the molecular weights of the inulin and sinistrin samples studied. However, inulin molecules turned out to be about 20% longer than sinistrin molecules, giving rise to the interpretation that inulin is less compact.

(b) A comparison of s.a.x.s. data with model calculations leads to the postulation of a rather elongated helical structure for inulin in aqueous solution. This hypothesis is further supported by the X-ray diffraction spectra of inulin, which closely correspond to the X-ray diffraction spectra of anhydrous V-amylose[17].

(c) In the case of sinistrin the ratio R_g/R_h is 0.8, which is close to the theoretical value for a spherical molecule. This finding is also a proof that the polydispersity is too low to affect the ratio R_g/R_h. For inulin R_g/R_h is 0.92. This clearly indicates a deviation from a sphere.

(d) The hydration of sinistrin turns out to be higher than that of inulin. This could explain the better solubility of sinistrin.

All these facts show a distinct difference between the structures of inulin and sinistrin, even at comparable molecular weights for the two polysaccharides. Thus the utilization of inulin and sinistrin as basic models for linear and branched polysaccharides, respectively, appears to be reasonable.

ACKNOWLEDGMENT

We are much indebted to E. Nitsch for providing the sinistrin sample.

REFERENCES

1 O. KANDLER AND H. HOPF, in F. A. LOEWUS AND W. TANNER (Eds.), *Encyclopedia of Plant Physiology*, New Series, Vol. 13A, Springer-Verlag, Berlin, 1982, pp. 349–383.
2 E. NITSCH, W. IWANOV, AND K. LEDERER, *Carbohydr. Res.*, 72 (1979) 1–12.

3 A. FUCHS, Thesis, University of Delft, 1959.
4 D. BIRKHED, K.-G. ROSELL, AND K. GRANATH, *Arch. Oral. Biol.*, 24 (1979) 53–61.
5 W. PRAZNIK AND R. H. F. BECK, *Agric. Biol. Chem.*, 51 (1987) 1593–1599.
6 J. EDELMAN AND T. G. JEFFORD, *New Phytol.*, 67 (1968) 517–531.
7 E. MIDDLETON, *J. Membr. Biol.*, 34 (1977) 93–101.
8 W. PRAZNIK AND R. H. F. BECK, *J. Chromatogr.*, 348 (1985) 187–197.
9 A. C. OUANO AND W. KAYE, *J. Polym. Sci., Polym. Chem. Ed.*, 12 (1974) 1151–1162.
10 R. C. JORDAN, *J. Liq. Chromatogr.*, 3 (1980) 439–464.
11 W.-D. EIGNER, in D. B. SATELLE, W. LEE, AND B. R. WARE (Eds.), *Biomedical Applications of Laser Light Scattering*, Elsevier, Amsterdam, 1982, pp. 403–408.
12 D. E. KOPPEL, *J. Chem. Phys.*, 57 (1972) 4814–4820.
13 O. GLATTER AND O. KRATKY (Eds.), *Small Angle X-ray Scattering*, Academic Press, New York, 1982.
14 O. GLATTER, *J. Appl. Crystallogr.*, 10 (1977) 415–421.
15 C. F. PHELPS, *Biochem. J.*, 95 (1965) 41–47.
16 O. GLATTER, *Acta Phys. Austr.*, 52 (1980) 234–256.
17 R. H. F. BECK, Thesis, Universität für Bodenkultur, Vienna, 1987.